

Interprétation avancée des calculs premiers principes des phonons par SIESTA

Andrei Postnikov



UNIVERSITÉ
DE LORRAINE

LCP-A2MC (Metz)
Institut Jean Barriol

GDR "Modélisation des matériaux"
21 février 2013
Marseille

Modélisation au sein de LCP-AM2C: périmètre, noms et chiffres

Laboratoire de Chimie et Physique – Approche Multi-Echelles des Milieux Complexes, résultant de la fusion (janvier 2012) des ex-laboratoires/équipes suivantes:

- Equipe Biophysique Statistique du LPMC (Laboratoire de Physique Moléculaire et Collisions);
- LPMD (Laboratoire de Physique des Milieux Denses);
- LSMCL (Laboratoire de Spectrométrie de Masse et Chimie Laser);
- LCME (Laboratoire de Chimie et Méthodologie pour l'Environnement).

Thèmes principaux de la recherche:

- 1) ‘Ordre-désordre/auto-organisation’ (Rhéophysique des colloïdes, désordre d’alliage dans les systèmes atomiques);
- 2) ‘Chimie durable et environnement’
(Contaminants et Dépollution, gestion durable des ressources).

46 enseignants-chercheurs sur les sites de Metz (Institut de Chimie et Physique, 1 Bd Arago, Technopôle) et Saint-Avold (IUT de Moselle-Est).



Michaël BADAWI

*Chimie quantique, adsorption, catalyse, surfaces, sûreté nucléaire

Logiciels commerciaux pour calculs ab initio:
VASP (structures périodiques);
Gaussian (moléculaires)

Journal of Catalysis 282 (2011) 155–164

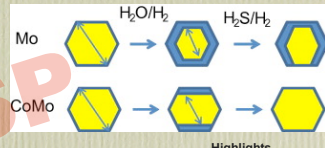
Contents lists available at ScienceDirect
Journal of Catalysis
journal homepage: www.elsevier.com/locate/jcat

ELSEVIER

Effect of water on the stability of Mo and CoMo hydrodeoxygenation catalysts: A combined experimental and DFT study

M. Badawi^a, J.F. Paul^a, S. Cristol^a, E. Payen^a, Y. Romero^b, F. Richard^b, S. Brunet^b, D. Lambert^c, X. Portier^d, A. Popov^e, E. Kondratieva^f, J.M. Goupil^c, J. El Fallah^c, J.P. Gilson^c, L. Mariet^c, A. Travert^{c,h}, F. Maugé^c

^a Institut de Génierie et de Mécanique des Solides, Institut de Sciences et Techniques de l'INRS, 3900 Avenue du Boisé, Québec, Québec, Canada G1R 0A6, Canada
^b Laboratoire de Catalyse en Chimie Organique, Université de Bruxelles (UCL), Avenue Princesse Élisabeth 30, 1050 Brussels, Belgium
^c Total Petrochemical Research Park, Zone Industrielle C, B-1161 JELLOU, Belgium
^d CMAP, ENSEIRB-MAThys, Université de Bordeaux, CNRS, INSA, 16 Boulevard du Maréchal Juin, 33400 Gars, France
^e Laboratoire Condens et Spectroscopie, ENSEIRB-MAThys, Université de Bordeaux, CNRS, 16 Boulevard du Maréchal Juin, 33400 Gars, France



Highlights

- Impact of H₂O on Mo and CoMo sulfide catalysts during HDO of phenolic compounds.
- Non-promoted Mo catalysts are more sensitive toward water due to SO exchanges.
- Co improves the activity (promotion) and stability of the active phase (passivation).

Computational and Theoretical Chemistry 960 (2012) 194–206

Contents lists available at SciVerse ScienceDirect
Computational and Theoretical Chemistry
journal homepage: www.elsevier.com/locate/comptoc

ELSEVIER

Ab initio calculations and iodine kinetic modeling in the reactor coolant system of a pressurized water reactor in case of severe nuclear accident

Bertrand Kerri^{a,c}, Sébastien Canneaux^{b,c}, Florent Louis^{b,c}, Julien Trinca^{a,c}, Frédéric Cousin^{a,c}, Michael Badawi^{a,c}, Laurent Cantrel^{a,c}

^a Institut de Radioprotection et de Sûreté Nucléaire, IRPhEN/CNRS, Centre de Gif-sur-Yvette, F91-3133 Suresnes Cedex, France
^b Physicochimie des Procédés de Confection et de l'Emballage (PCCE), UMR 8522 CNRS/INRA/Université Paris-Sud / Sciences et Technologies, Cité scientifique, Bât C1/CS, 91393

Highlights

- Thermodynamic and kinetic parameters are calculated using ab initio molecular orbital methods.
- Calculated reaction enthalpies at 0 K are close to their literature counterparts.
- Rate constants are calculated from 300 to 2500 K and compared to the available literature data.
- Iodine kinetic model is developed.
- Simulations with the ASTEC software are performed in the framework of nuclear safety.

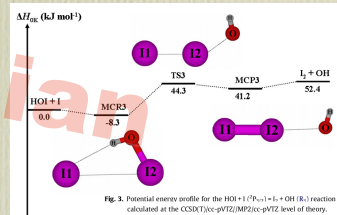


Fig. 3. Potential energy profile for the HOI + I ($\text{I}^2\text{P}_{3/2}$) reaction calculated at the CCSCT(cc-pVTZ)/MP2(cc-pVTZ) level of theory.



Jean-Marc BOMONT

- Relation structure moléculaire – propriétés macroscopiques: les gaz rares etc.
- Etude de colloïdes (dynamique moléculaire, Monte-Carlo), de la thermodynamique statistique et de la méthode des équations intégrales auto-cohérentes.
- Propriétés optiques non-linéaires de fluides simples.
- Simulation hors équilibre (NEMD).
- Développement de potentiels interatomiques analytiques de métaux liquides (Hg).

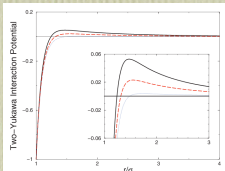


FIG. 1. The 2Y interaction potential. Full line: $K_2/K_1=0.1$; dashed line: $K_2/K_1=0.05$; dotted line: $K_2/K_1=0.01$. All potentials are rescaled in such a way that the depth of the potential well $\omega=K_1-K_2$ is equal to minus one. The inset contains a magnification of the region around the repulsive barrier.

Logiciels utilisés “maison” (Fortran 77 ou 90, séquentiels):
Dynamique moléculaire classique; Monte Carlo

THE JOURNAL OF CHEMICAL PHYSICS 132, 184508 (2010)

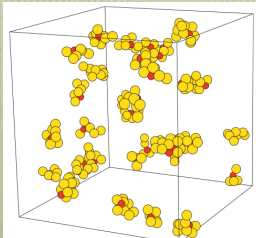
Temperature study of cluster formation in two-Yukawa fluids

Jean-Marc Bomont,^{1,a)} Jean-Louis Bretonnet,¹ and Dino Costa²

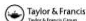
¹Laboratoire de Physique des Milieux Denses, Université de Metz, 1 Bd. Arago, 57 078 Metz, France

²Dipartimento di Fisica, Università degli Studi di Messina, Viale F. Stagno d’Alcontres 31, 98166 Messina, Italy

(Received 10 December 2009; accepted 7 April 2010; published online 12 May 2010)



Molecular Physics
Vol. 109, Nos. 23–24, 10 December–20 December 2011, 2845–2853



INVITED ARTICLE

Theoretical description of cluster formation in two-Yukawa competing fluids

D. Costa^{a*}, C. Caccamo^a, J.-M. Bomont^b and J.-L. Bretonnet^b

^aDipartimento di Fisica, Università degli Studi di Messina, Viale F. Stagno d’Alcontres 31, 98166 Messina, Italy;

^bLaboratoire de Physique des Milieux Denses, Université Paul Verlaine, 1 Bd. Arago, 57078 Metz, France

(Received 30 June 2011; final version received 28 July 2011)

Snapshot of an equilibrated sample at $T^*=0.46$ with $K_2/K_1=0.10$.
For the clarity sake, only particles involved in the formation of clusters
are shown. Red particles represent the seeds of the compact structures.



Réné MESSINA

* Cristallisation de colloïdes chargés binaires

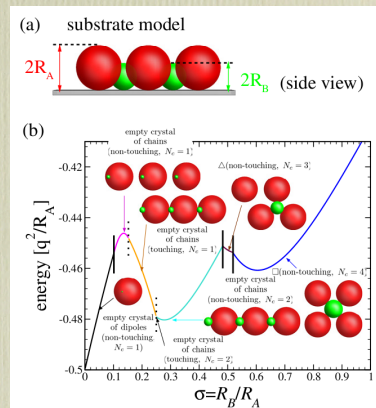
Logiciels utilisés “maison” (Fortran 77 ou 90, sequentiels)
pour faire :

- Monte Carlo
- Dynamique brownienne ou de Langevin (équilibre & hors équilibre)
- Minimisation d'énergie sur réseaux cristallins
- Résolution d'équations différentielles non linéaires (Poisson-Boltzmann)

Configuration “idéale” du calcul: 40-50 noeuds; 1 Go RAM / CPU



Fig. 3: (Colour on-line) Stable structures of oppositely charged spheres *vs.* their size asymmetry $\sigma = R_B/R_A$ in the substrate model, where all sphere surfaces touch the same plane: a) side view, b) (scaled) energy per ion. Discontinuous transitions between the structures are indicated by a solid bar. Continuous transitions are denoted by a broken bar. Bottom views of the unit cells of the corresponding stable phases are displayed, where the big (small) spheres have a radius R_A (R_B).





Martin Mickaël MULLER

*Propriétés géométriques des membranes biologiques

Codes open source: libMesh (mesh support),
VTK (visualisation), OpenMPI



A LETTERS JOURNAL EXPLORING
THE FRONTIERS OF PHYSICS

EPL, 97 (2012) 68008
doi: 10.1209/0295-5075/97/68008

March 2012

www.epljournal.org

Morphogenesis of membrane invaginations in spherical confinement

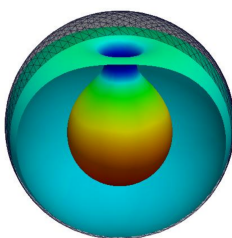
O. KAHRAMAN¹, N. STOOP² and M. M. MÜLLER¹

¹ Équipe BioPhysStat, ICPMB-FR CNRS 2843, Université de Lorraine - 1, boulevard Arago,
F-57070 Metz, France, EU

² Computational Physics for Engineering Materials, ETH Zurich - Schafmattstr. 6, HIF,
CH-8093 Zurich, Switzerland

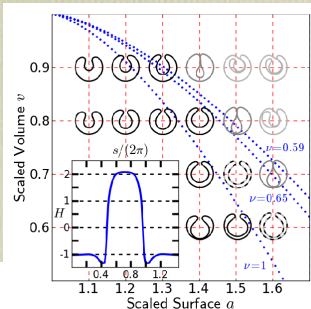
received 12 January 2012; accepted in final form 20 February 2012

published online 22 March 2012



a geometrical phase diagram
of fluid membrane invaginations:

Numerical equilibrium solution for a membrane (smooth surface) inside a spherical container (black mesh) with scaled area $a = 1.2$ and scaled volume $v = 0.8$. The membrane bulges inward and forms an invagination reminiscent of a light bulb.





Jean-François WAX

- Dynamique des liquides (surtout des métaux)
- Propriétés statiques et dynamiques, diffusion, viscosité
- Diagrammes de phase densité - température

Dynamique Moléculaire classique (code maison) et ab initio (VASP)

PHYSICAL REVIEW B 83, 144203 (2011)

Multiscale study of the influence of chemical order on the properties of liquid Li-Bi alloys

J.-F. Wax

Laboratoire de Physique des Milieux Denses, Université Paul Verlaine - Metz, 1, Boulevard F. D. Arago, F-57078 Metz Cedex 3, France

M. R. Johnson

Institut Laue Langevin, 6 rue Jules Horowitz, F-38042 Grenoble Cedex 9, France

L. E. Bove

Physique des Milieux Denses, IMPMC, CNRS-UMR 7590, Université Pierre et Marie Curie, F-75252 Paris, France

M. Mihalkovič

Institute of Physics, Slovak Academy of Sciences, Dubravská cesta 9, 84511 Bratislava, Slovakia
(Received 22 July 2010; revised manuscript received 22 November 2010; published 13 April 2011)

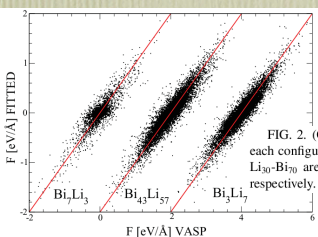
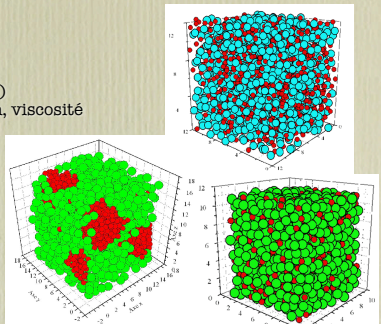


FIG. 2. (Color online) Fitted forces versus *ab initio* ones for each configuration considered. Data corresponding to Li₅₇-Bi₄₃ and Li₃₀-Bi₇₀ are shifted by 2 and 4 eV/Å along the horizontal axis, respectively.



L'ordre chimique dans un liquide:
aléatoire; homocoordonné; hétéocoordonné...

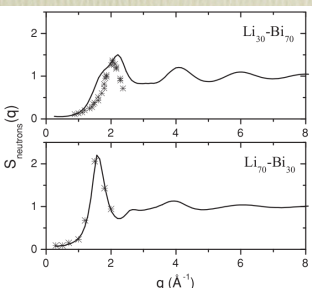


FIG. 6. Total structure factors for neutrons (full line: simulation; symbols: experiment).



Hong XU

- Dynamique moléculaire classique et ab initio des liquides complexes
- Transitions de phase dans des liquides; propriétés interfaciales

Logiciels utilisés “maison” et LAMMPS (C++, MPI)

PHYSICAL REVIEW E **79**, 041501 (2009)

Structure and dynamics of cylindrical micelles at equilibrium and under shear flow

C.-C. Huang,¹ J.-P. Ryckaert,² and H. Xu³

¹Institut für Festkörperforschung, Forschungszentrum Jülich GmbH, 52425 Jülich, Germany

²Physique des Polymères, Université Libre de Bruxelles, Campus Plaine, CP 223, B-1050 Brussels, Belgium

³Laboratoire de Physique des Milieux Denses, Université Paul Verlaine-Metz, 1 Boulevard Arago, 57078 Metz Cedex 3, France

(Received 28 November 2008; published 9 April 2009)

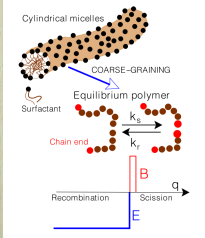


Figure 1: Some surfactant molecules in solution self-assemble and form long wormlike micelles which continuously break and recombine. Their mass distribution is, hence, in thermal equilibrium and they present an important example of the vast class of systems termed “equilibrium polymers”[1].

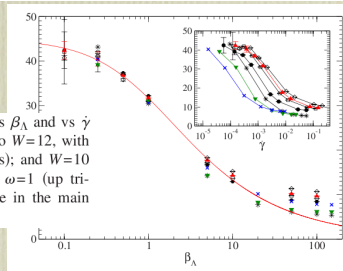


FIG. 8. (Color online) The extinction angle χ_O vs β_A and vs $\dot{\gamma}$ (inset), for both semidilute cases. Data correspond to $W=12$, with $\omega=0.02$ (cross), $\omega=0.1$ (down triangles), $\omega=1$ (stars); and $W=10$ with $\omega=0.1$ (filled circles), $\omega=0.5$ (open squares), $\omega=1$ (up triangles), $\omega=5$ (open diamonds). The continuous line in the main figure corresponds to the empirical law.



Andrei POSTNIKOV

- Structure électronique ab initio (DFT): solides, liquides, molécules
- Dynamique de réseau des semiconducteurs mixtes

Logiciels utilisés:

- SIESTA (pseudopotentiels, fonctions de base numériques)
- WIEN2k (“tous électrons”)

$\sim 10^2 - 10^3$ atomes, périodiques ou isolés (SIESTA)

Coordination Chemistry Reviews 253 (2009) 2387–2398

Contents lists available at ScienceDirect

Coordination Chemistry Reviews

journal homepage: www.elsevier.com/locate/CCR

Review

STM spectroscopy of magnetic molecules

K. Petukhov^a, M.S. Alam^a, H. Rupp^a, S. Strömsdörfer^a, P. Müller^{a,*}, A. Scheurer^b, R.W. Saalfrank^b, J. Kortus^c, A. Postnikov^d, M. Ruben^e, L.K. Thompson^f, J.-M. Lehn^g

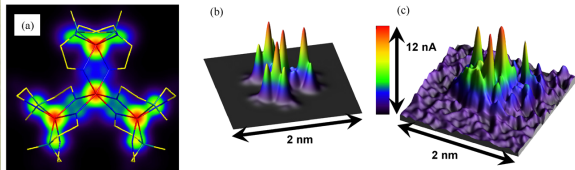


Fig. 13. (a) Color coded map of the DFT calculated electron density of **3** within an energy window between E_F and -0.95 eV in superposition with the crystal structure data (sticks), the scale is 1.2 nm \times 1.2 nm. (b) 3D representation of the DFT electron density map; (c) 3D representation of the central section of the experimental CITS map taken at -0.918 V.

Phys. Status Solidi A **206**, No. 5, 1020–1033 (2009) / DOI 10.1002/pssa.20081217

Impurity vibration modes in II–VI and III–V mixed semiconductors

Andrei Postnikov^a, Olivier Pagès^a, Jihane Souhabi^a, Ayoub Nassour^a, and Joseph Hugel^b

Laboratoire de Physique des Milieux Denses, Paul Verlaine University, 1 Bd Arago, 57078 Metz, France

Received 1 September 2008, revised 24 November 2008, accepted 26 January 2009

Published online 25 March 2009

pss
status
solidi
physica
www.pss-a.com
applications and materials science

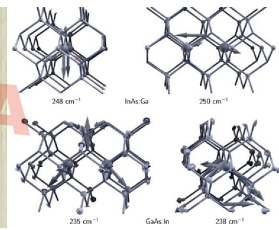


Figure 4 Calculated vibration patterns in selected zone-center coupled-impurity modes. Top row: Ga (large spheres) impurities in InAs; the modes at 248 cm^{-1} and 250 cm^{-1} . Bottom row: In (large spheres) impurities in GaAs; the modes at 235 cm^{-1} and 238 cm^{-1} .

SIESTA way to phonons

① $\mathbf{q} = 0$ only needed? \rightarrow frozen phonons.

$$m_\alpha \ddot{u}_\alpha^i = - \sum_{\beta}^N \sum_j^3 F_{\alpha\beta}^{ij} u_{\beta}^j$$

② Dispersion needed? \rightarrow construct a supercell, look at forces induced everywhere.

③ Fourier-transform the force constants;
diagonalize for any \mathbf{q} needed.

$$\begin{pmatrix} & & \vdots \\ \frac{F_{ss'}^{ij}(\mathbf{q})}{\sqrt{m_s m_{s'}}} - \omega^2 \delta_{ss'} \delta_{ij} & & \\ & & \vdots \end{pmatrix} \begin{pmatrix} u_{s' \mathbf{q}}^j \sqrt{m_{s'}} \\ \vdots \end{pmatrix} = 0$$

- ④ A case of solid solution, e.g., mixed semiconductors: supercell anyway; exact lattice periodicity is broken anyway \rightarrow case 1.
- ⑤ However, a large supercell contains folded-in $\mathbf{q} \neq 0$ modes, and many “long” eigenvectors contain a lot of information. Try to extract it.

\mathbf{q} -resolved modes density

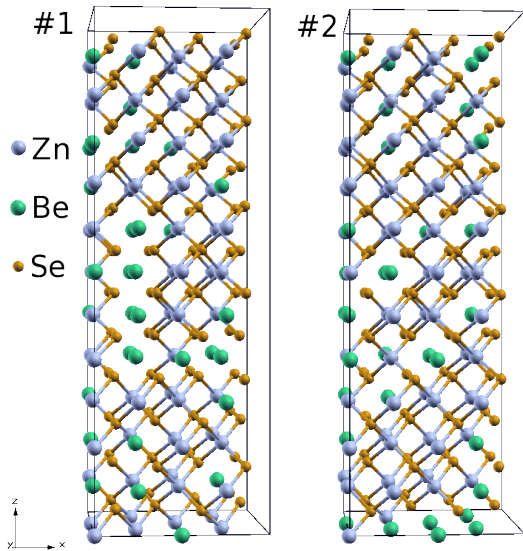
In solid solutions, where topological disorder destroys an exact crystal periodicity, the projection of phonon eigenvectors taken along with a $\exp(i\mathbf{q}\mathbf{R})$ plane wave may help to reveal somehow a smeared $\omega(\mathbf{q})$ dispersion trends in a form of “spectral function”:

$$I_N(\omega, \mathbf{q}) = \sum_i \left| \sum_{\alpha \in N} \mathbf{A}_i^\alpha(\omega) e^{i\mathbf{q}\mathbf{R}_\alpha} \right|^2 \delta(\omega - \omega_i).$$

It amplifies the weights of vibrations in which similar atoms move in phase with a given \mathbf{q} -wave throughout the crystal, and suppresses the movements whose phase are at random with such wave. In particular, the $\mathbf{q}=0$ projection amplifies the “prototype” zone-center TO mode of zincblende crystal, the quasi rigid movement of the cation sublattice against the anion one:

$$I_N(\omega, \mathbf{q}=0) = \sum_i \left| \sum_{\alpha \in N} \mathbf{A}_i^\alpha(\omega) \right|^2 \delta(\omega - \omega_i).$$

q-resolved modes density: an example of (Zn,Be)Se

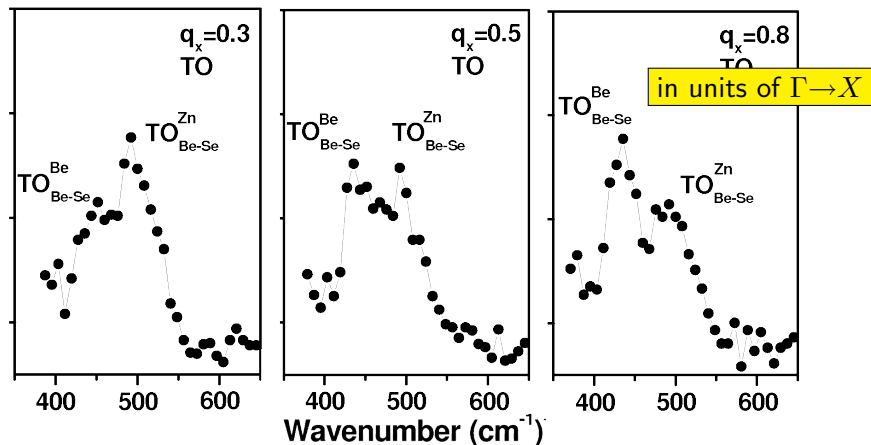


- **Motivation:** probing the “1-bond – 2-mode” behaviour away from the Brillouin zone center.
- Solid solution is simulated by **Special Quasirandom Supercells**.
- Two different ones were tried, of $64 \times 3 = 192$ atoms (long in one dimension, in order to well probe the dispersion).
- **Experimental situation:** inelastic neutron scattering (Mala N. Rao – Tista Basak – S.L. Chaplot *et al.*); tentative synthesis by Olivier Pags (under preparation)

q -resolved modes density: an example of (Zn,Be)Se

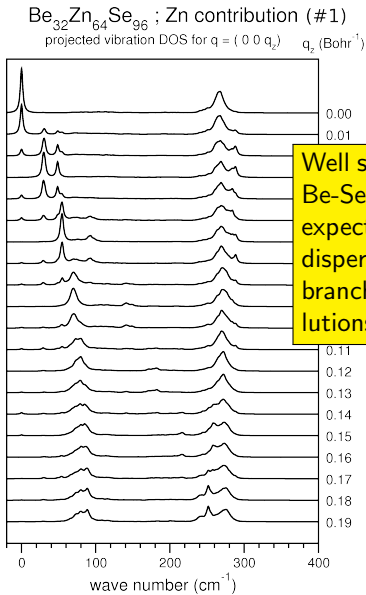
Experimental situation:

inelastic neutron scattering (Mala N. Rao – Tista Basak – S.L. Chaplot *et al.*)



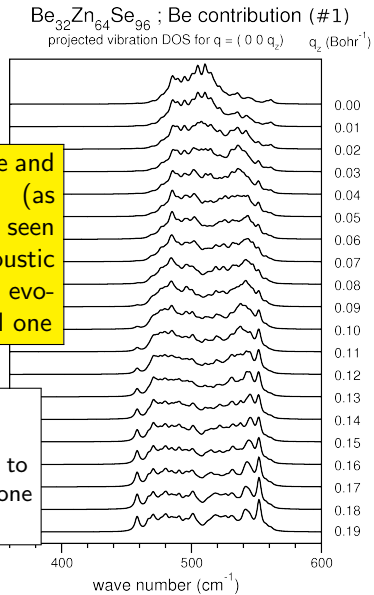
We know this situation at $q=0$, and assign the labels correspondingly.
Would an *ab initio* simulation confirm this?

q-resolved modes density: an example of (Zn,Be)Se

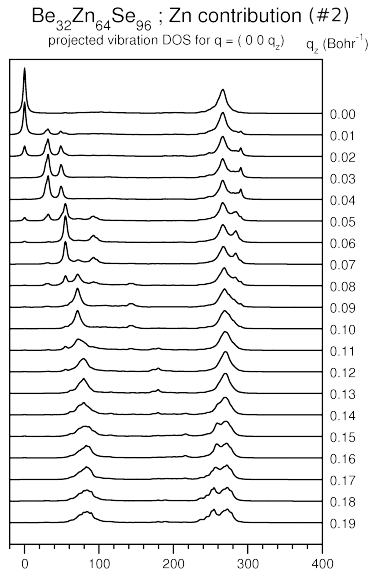
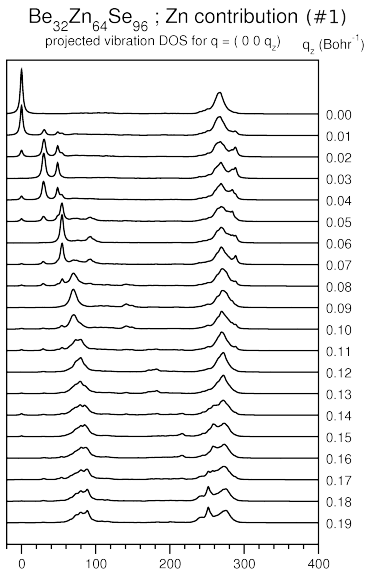


Well separated Zn-Se and Be-Se vibrations... (as expected). A clearly seen dispersion in the acoustic branch... and some evolutions in the optical one

← abs. units.
The last value
≈ corresponds to
the Brillouin zone
boundary (X).

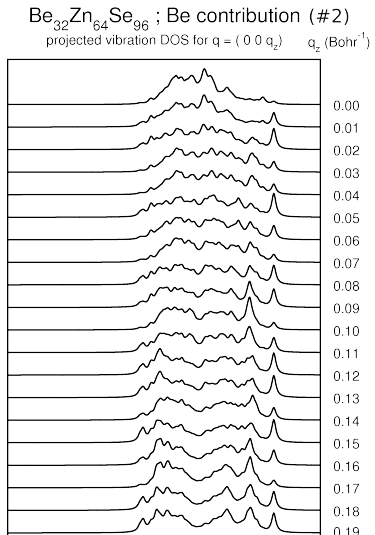
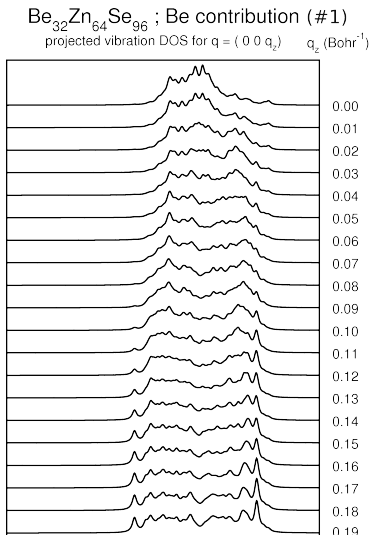


q -resolved modes density: an example of (Zn,Be)Se



Check whether the trends depend much on the supercell... Seems not to be the case!

q -resolved modes density: an example of (Zn,Be)Se

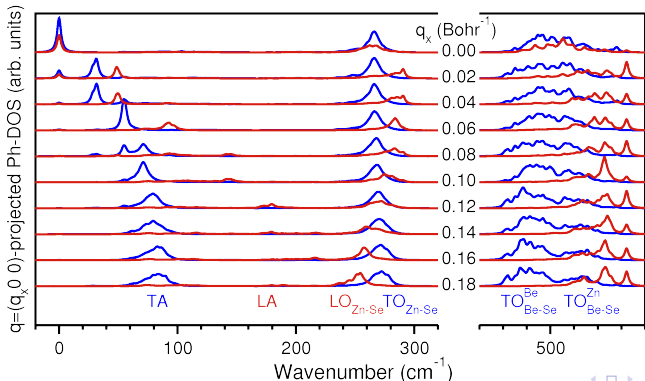


More pronounced are supercell-dependent differences in the Be-Se domain (Be is in minority and worse “averaged”). Nevertheless, the two-mode behaviour persists.

Projecting into Longitudinal and Transversal components

$$I_{\aleph}^L(\omega, \mathbf{q}) = \sum_i \left| \sum_{\alpha \in \aleph} \left(\frac{\mathbf{q}}{|\mathbf{q}|} \cdot \mathbf{A}_i^\alpha e^{i\mathbf{q}\mathbf{R}_\alpha} \right) \right|^2 \delta(\omega - \omega_i);$$

$$I_{\aleph}^T(\omega, \mathbf{q}) = \sum_i \left| \sum_{\alpha \in \aleph} \left[\mathbf{A}_i^\alpha - \frac{(\mathbf{q} \cdot \mathbf{A}_i^\alpha)}{|\mathbf{q}|} \right] e^{i\mathbf{q}\mathbf{R}_\alpha} \right|^2 \delta(\omega - \omega_i).$$



An example
of $(\text{Zn},\text{Be})\text{Se}$:
note the crossing of
LO and TO branches
with q
in the ZnSe domain.

Symmetry considerations for phonons

"Conventional" approach to symmetry of vibrations (\rightarrow "frozen phonons"):
Symmetry coordinates (along to irred.rep. of the space group in question):
 $S_t = \sum_j B_{tj} u_j$. Classical kinetic and potential energy:

$$\begin{aligned} T &= \sum_i \frac{m_i \dot{u}_i^2}{2} = \sum_{tt'i} (B^{-1})_{it} (B^{-1})_{it'} \frac{m_i}{2} \dot{S}_t \dot{S}_{t'}, \\ U &= \frac{1}{2} \sum_{tt'} F_{tt'} S_t S_{t'}. \end{aligned}$$

Lagrangian equation of motion:

$$\sum_{t'} \left[\sum_i (B^{-1})_{it} m_i (B^{-1})_{it'} \ddot{S}_{t'} + (F_{tt'} + F_{t't}) S_{t'} \right] = 0$$

with $G_{tt'} = \sum_i B_{it} m_i^{-1} B_{it'}$ – kinetic energy matrix

$$[\mathbf{F} - \omega^2 \mathbf{G}^{-1}] \mathbf{A} = 0, \quad \text{or} \quad (\mathbf{G}^{1/2} \mathbf{F} \mathbf{G}^{1/2} - \omega^2) \mathbf{A} = 0.$$

\rightarrow eigenvalues and eigenvectors within each irred.rep. independently.

Symmetry-projected density of modes

“Post-processing”: first obtain eigenvector of each mode (no symmetry constraints), *then* project it according to irred.reps. *Advantage:* works also for solid solutions and otherwise “approximate symmetry”.

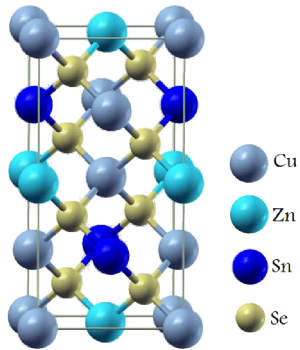
$$I_{\aleph}^{\nu}(\omega) = \sum_i \left| \sum_{\alpha \in \aleph} \mathbf{A}_i^{\alpha} \mathbf{S}_i^{\alpha\nu} \right|^2 \delta(\omega - \omega_i).$$

$\mathbf{S}_i^{\alpha\nu}$: projection vectors (in the 3-dim. space of individual atom displacements); ν : irreducible representation of underlying (or, presumed, if “approximative”) space group; i : mode index; α : atom index.

Where to get $\mathbf{S}_i^{\alpha\nu}$ (for example...) :

go to <http://www.cryst.ehu.es> (Bilbao crystallographic server), specifically to its SAM section <http://www.cryst.ehu.es/rep/sam.html>, choose the space group, select a Wyckoff position, select “Show”, go to “Mechanical representation” and again select “Show”.

An example: kesterite-type Cu₂ZnSnSe₄ (space group $I\bar{4}$)



Symmetry coordinates in different vibration modes constructed from individual Cartesian displacements $\pm(X, Y, Z)$ of anions

Modes	Anion sites: $(0\ 0\ 0)^+$; $(\frac{1}{2}\ \frac{1}{2}\ \frac{1}{2})^+$			
	$(\frac{1}{4}\ \frac{3}{4}\ \frac{1}{8})$	$(\frac{3}{4}\ \frac{1}{4}\ \frac{1}{8})$	$(\frac{3}{4}\ \frac{3}{4}\ \frac{7}{8})$	$(\frac{1}{4}\ \frac{1}{4}\ \frac{7}{8})$
$A\ #1$	Y	$-Y$	X	$-X$
$A\ #2$	$-X$	X	Y	$-Y$
$A\ #3$	$-Z$	$-Z$	Z	Z
$B\ #1$	Y	$-Y$	$-X$	X
$B\ #2$	$-X$	X	$-Y$	Y
$B\ #3$	Z	Z	Z	Z
$(E^1 + E^2)\ #1$	X	X	—	—
$(E^1 + E^2)\ #2$	Y	Y	—	—
$(E^1 + E^2)\ #3$	Z	$-Z$	—	—
$(E^1 - E^2)\ #1$	—	—	Y	Y
$(E^1 - E^2)\ #2$	—	—	X	X
$(E^1 - E^2)\ #3$	—	—	$-Z$	Z

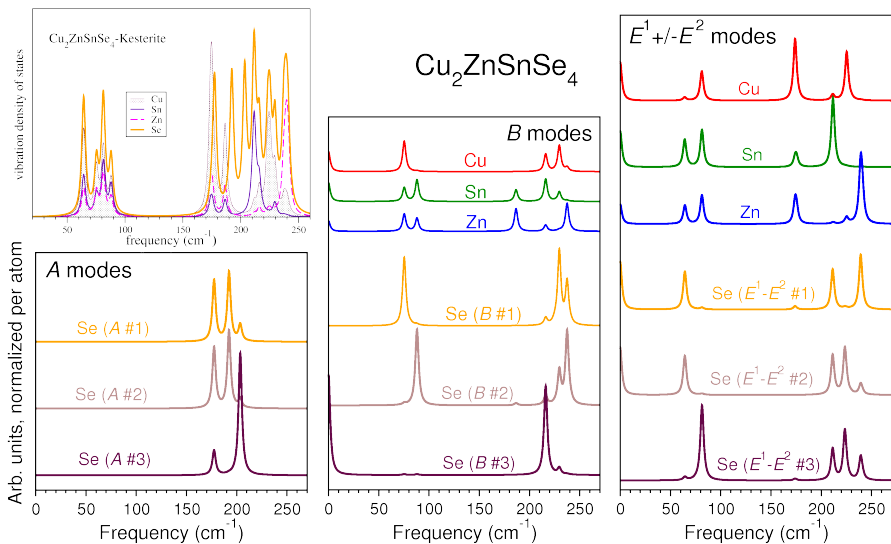
Decomposition of vibration modes according to symmetries

Wyckoff positions	Irred. representations			(sums up to 8 at. $\times 3 = 24$)
	A	B	E	
Cu (2a)	1	1	1	$1+1\times 2 = 3$
Sn (2b)	1	1	1	$1+1\times 2 = 3$
Cu (2c)	1	1	1	$1+1\times 2 = 3$
Zn (2d)	1	1	1	$1+1\times 2 = 3$
Se (8g)	3	3	3	$3+3+3\times 2 = 12$

Symmetry coordinates (as above) for cations

Modes	Wyckoff positions			
	(2a)	(2b)	(2c)	(2d)
B	Z	Z	Z	Z
$(E^1 + E^2)$	X	X	X	X
$(E^1 - E^2)$	Y	Y	Y	Y

CZTSe: Γ -vibrations and symmetry analysis



NB: within modes of the same symmetry block, and between partners of the same irreducible representation, the decomposition is ambiguous!

Cu_2SnSe_3 vs. $\text{Cu}_2\text{ZnSnSe}_4$: structure and phonons

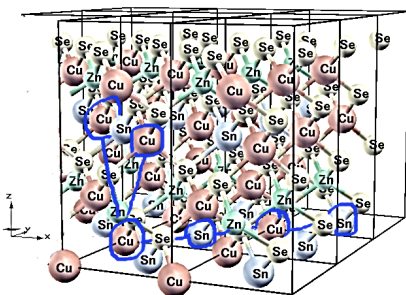
$\text{Cu}_2\text{ZnSnSe}_4$ (CZTS) of kesterite-type structure (bct)

is a promising material for photovoltaics.

Cu_2SnSe_3 (CTSe) is one of “secondary phases” (\rightarrow monoclinic)

frequent in the phase diagram of Cu–Sn–Se, useless for photovoltaics.

The two structures correspond to different cation arrangement on the same underlying (zincblende) lattice. They are indistinguishable in X-ray diffraction; our motivation was to pinpoint existing differences in their vibration spectra (in view of identifying possible “vibrational fingerprints”).



- monoclinic b axis along the [110] diagonal of the basal plane of kesterite;
- a , c vectors are valid lattice vectors of kesterite: $[\frac{1}{2} \frac{1}{2} \pm \frac{1}{2}]$;
- 3× stapling of CZTSe kesterite (along monoclinic b) matches 2× of CTSe

Density of modes at $\mathbf{q} = 0$

of supercell

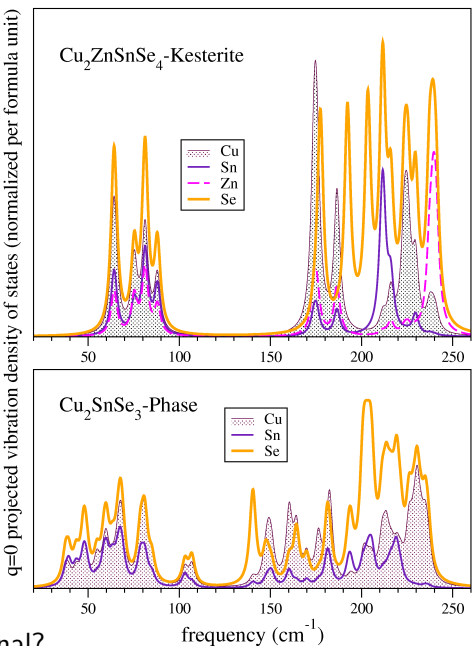
N atoms $\rightarrow 3N$ modes ν ,
frequencies ω_ν , eigenvectors $A_\nu^{i\alpha}$
(i : cartesian x,y,z ;
 α : atom of species \aleph).

$$I_\aleph(\omega) = \sum_{\nu} \sum_{\alpha \in \aleph} \sum_i [A_\nu^{i\alpha}]^2 \delta(\omega - \omega_\nu)$$

CZTSe: 8 at. / primitive cell,
CTSe: 24 at. / primitive cell

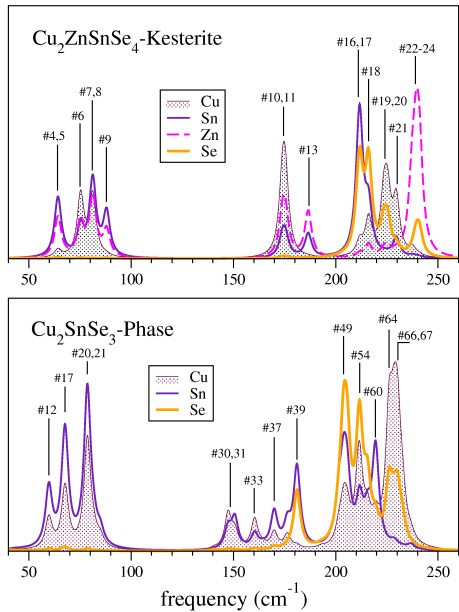
Formally, all are zone-center modes,
yet the spectrum is more rich
(as of a supercell...)

Do all these modes give a Raman signal?



Density of modes; q-projection

q=0 projected vibration density of states (normalized per atom)



A “zincblende-like” q-projection

$$I_{\aleph}(\omega) = \sum_{\nu} \sum_{\alpha \in \aleph} [A_{\nu}^{i\alpha} e^{i\mathbf{R}_{\alpha}\mathbf{q}}]^2 \delta(\omega - \omega_{\nu})$$

(q=0 in the plot on the left):

Emphasizes “all cations against all anions” patterns (but not only, since projection for each species is done independently).

This recovers some similarity in spectra, and underlines the splitting of modes into three groups.

More in

J.Appl.Phys. **112**, 033719 (2012);
Phys.Rev.B **82**, 205204 (2010).

Vibration entropy (for phase diagrams calculations)

In a system of harmonic oscillators with mode density $g(\omega)$ obeying the Bose-Einstein statistics:

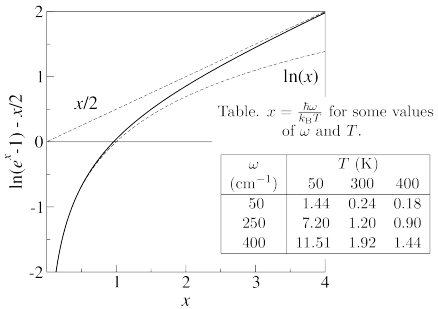
$$\text{free energy } F = k_B T \int_0^{\omega_{\max}} \left[\ln(e^x - 1) - \frac{x}{2} \right] g(\omega) d\omega \quad \text{with } x = \frac{\hbar\omega}{k_B T};$$

$$S = -\frac{\partial F}{\partial T} = k_B \int_0^{\omega_{\max}} \left[\frac{x}{e^x - 1} - \ln(1 - e^{-x}) \right] g(\omega) d\omega.$$

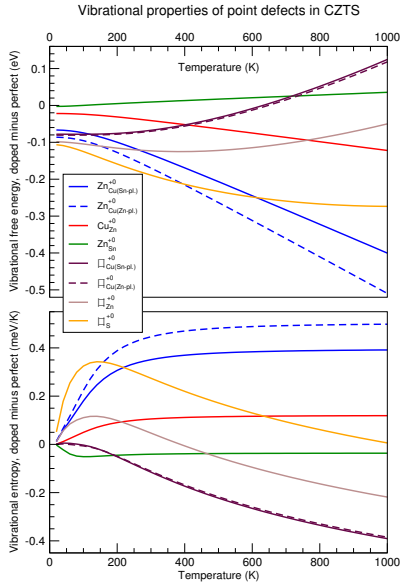
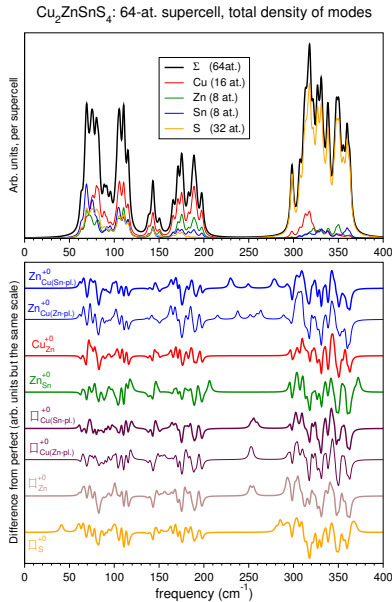
In a large supercell, $\mathbf{q} = 0$ discrete spectrum samples the continuous density of modes:

$$g(\omega) \approx \sum_{\alpha} \delta(\omega - \omega_{\alpha}).$$

The supercell may include defects with their (possibly) localized vibration modes.



Vibration entropy calculations: $\text{Cu}_2\text{ZnSnS}_4$ with point defects



Conclusion

- Calculated phonon eigenvectors contain very rich information which is often neglected, or used in cumulated form only. However, it can be conveniently extracted by applying a projection technique (with respect to properties of immediate interest).
- Projections to mention are onto atom / atom type (obvious), but also (less obvious) onto a \mathbf{q} -vector and onto a symmetry block (irreducible representation of the space group).
- Projection technique can also be applied to the study of *solid solutions*, when the nominal symmetry relations (with respect to translations / rotations) are not exactly valid. Still, the trends can be revealed (e.g., dispersion relations in an alloy, a routine issue of discussion in experimental works).
- The above projection tools are readily available for post-processing of SIESTA results [ask andrei.postnikov@univ-lorraine.fr]; for other codes, at most, some modification of data format may be needed.